Doppler Effect of Nonlinear Waves and Superspirals in Oscillatory Media

Lutz Brusch,[1] Alessandro Torcini,[2,*] and Markus Bär[1,†]

[1]*MPI for Physics of Complex Systems, Nöthnitzer Strasse 38, D-01187 Dresden, Germany*
[2]*Istituto Nazionale di Ottica Applicata, Largo Enrico Fermi 6, I-50125 Firenze, Italy*

(Received 12 February 2003; published 5 September 2003)

Nonlinear waves emitted from a moving source are studied. A meandering spiral in a reaction-diffusion medium provides an example in which waves originate from a source exhibiting a back-and-forth movement in a radial direction. The periodic motion of the source induces a Doppler effect that causes a modulation in wavelength and amplitude of the waves (''superspiral''). Using direct simulations as well as numerical nonlinear analysis within the complex Ginzburg-Landau equation, we show that waves subject to a convective Eckhaus instability can exhibit monotonic growth or decay as well as saturation of these modulations depending on the perturbation frequency. Our findings elucidate recent experimental observations concerning superspirals and their decay to spatiotemporal chaos.

DOI: 10.1103/PhysRevLett.91.108302 PACS numbers: 82.40.Ck, 05.45.–a, 47.54.+r, 89.75.Kd

Introduction.—Periodic nonlinear waves are a trademark of nonequilibrium systems [1]. In one dimension (1D), they can appear in systems with periodic boundary conditions (BCs) as well as in open geometries, where BCs select a unique pattern [2]. In two dimensions (2D), rotating spiral waves are frequently observed. Therein, periodic waves emerge from the region of the spiral tip (core) and propagate in a radial direction. The aim of this paper is to investigate the effects of perturbing sources of nonlinear waves and their implications for the dynamics of spiral waves. We employ the complex Ginzburg-Landau equation (CGLE), which provides a universal description of spatially extended oscillatory systems near a supercritical Hopf bifurcation [3,4].

In this framework, we perturb a source of periodic waves in 1D by moving its position back and forth in space. This motion of the source leads to a modulation in amplitude, wavelength, and frequency of the emitted waves. We find that the modulation of the nonlinear waves is uniquely determined by the temporal period of the source motion in contrast to linear waves emitted by a moving source, where the source velocity is the relevant quantity. The richest scenario is found if the emitted waves are convectively Eckhaus unstable. If we consider a periodically moving source in the latter case, the modulations in amplitude and period of the waves may (i) get exponentially damped, (ii) saturate, or (iii) grow monotonic far away from the source depending on the frequency of the applied forcing.

Such a periodically moving source reproduces the radial dynamics of rotating spiral waves subject to external forcing [5] or to the frequently observed oscillatory instability termed ''meandering'' [6]. In 2D, the radial modulations caused by meandering lead to a second spiral superimposed on the simple rotating spiral; the resulting structure is called superspiral (see Fig. 1). Our fully nonlinear numerical analysis of coherent structures emitted by a moving source provides insight in the nonlinear behavior of superspirals and extends previous work limited to a linear approach [7]. Unbounded growth of the modulation will lead to occurrence of space-time defects in 1D and superspiral breakup in 2D, provided the system is sufficiently large. Experimental evidence of such behavior was found in the Belousov-Zhabotinsky (BZ) reaction [8]. Superspirals were first reported in experiments with strong external forcing near the spiral core [9].

Complex Ginzburg-Landau equation.—Consider a spatially extended oscillatory medium described by the complex Ginzburg-Landau equation [1,4]

$$\partial_t A = \mu A + (1 + ic_1)\Delta A - (1 - ic_3)|A|^2 A \qquad (1)$$

with $\mu = 1$. The complex field $A(r, t)$ gives the amplitude and phase of local oscillations depending on real coefficients c_1, c_3 determined by the underlying specific model at the onset of oscillations. Equation (1) exhibits plane wave solutions $A(r,t) = \sqrt{1-q^2}e^{i(qr-\omega t)}$ with $\omega = -c_3 + q^2(c_1 + c_3)$ in an infinite or periodic 1D medium

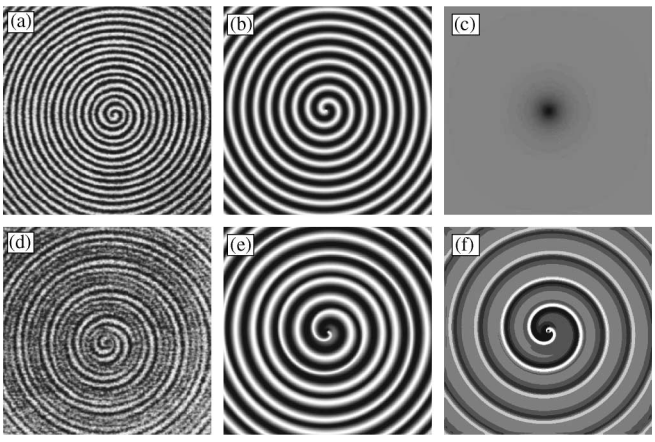

FIG. 1. Simple spiral waves (a)–(c) and superspirals (d)–(f) are observed in experiments (a),(d) of the BZ system [8] and in numerical simulations of the CGLE (1). (b),(e) show Re[A] and (c),(f) show $|A|$. (b),(c) $\mu = 1$ and (e),(f) inhomogeneous $\mu = 1 + 0.7\exp(-r^2/10)$. Other parameters are $c_1 = 3.5$, $c_3 = 0.34$, system size is 512×512.

with $\Delta = \partial_r^2$. For fixed control parameters, these waves become unstable if the wave number q is bigger than the Eckhaus wave number $q_E^2 = (1 - c_1c_3)/[2(1 + c_3^2) + 1 - c_1c_3]$. The plane waves represent a one-parameter family that is parametrized by the wave number q. A source of periodic waves at $r = 0$ is easily realized by applying the BCs

$$A(r = 0) = 0 \quad \text{and} \quad \partial_r A(r = L) = 0. \tag{2}$$

The specification of these BCs leads to the selection of a unique wave number q_S. In this case, the exact solution of the CGLE is of the form

$$A(r, t) = F(r)e^{i(f(r)-\omega t)}, \tag{3}$$

with the asymptotic behavior $df(r)/dr \to q_S$, $F(r) \to \sqrt{1 - q_S^2}$ for $r \to \infty$ (far field) and $df(r)/dr \sim r$, $F(r) \sim r$ for $r \to 0$ (near field). An analytic expression for q_S has been derived [2,10]

$$0 = (c_1 + c_3)q_S^2 + 3\alpha(c_1, c_3)q_S - c_3 - 2c_1\alpha(c_1, c_3)^2, \tag{4}$$

where α is a function of the control parameters c_1, c_3 [11].

In 2D, Eq. (1) with $\Delta = \partial_r^2 + 1/r\partial_r + 1/r^2\partial_\theta^2$ possesses rotating spiral solutions with $A = 0$ in the spiral core and in the far field a selected wave number q_S, which is similar to (4) as verified numerically [2,10]. Equation (4) allows one to discriminate if the source or the spiral core emits stable (Eckhaus unstable) wave trains with $q_S < q_E$ ($q_S > q_E$). Further analysis showed that the Eckhaus instability is of convective nature and becomes absolute for sufficiently large values of c_1 and c_3 [12]. At given parameters, we may define a wave number $q_A > q_E$ that characterizes absolutely unstable waves with $q > q_A$. In finite systems, spirals were found to be stable as long as $q_S < q_A$ [12,13].

Simulation results.—Here, we analyze the effects of an instability or of an external perturbation at the source or at the spiral core (meandering). We choose to perturb the source in Eq. (2) by varying its position r_S.

$$A(r \le r_S) = 0$$

with

$$r_S = R_S \cos(2\pi t/\tau) \quad \text{and} \quad \partial_r A(r = L) = 0 \tag{5}$$

is therefore used as a BC of Eq. (1) in 1D. The core motion of a meandering spiral can be viewed as a source moving along a circle in 2D. A projection onto a radial direction for a fixed angle yields a periodic back-and-forth motion. A sinusoidal motion as in Eq. (5) is expected near onset, where the normal form of meandering [14] provides a valid description. Hence, the BC in Eq. (5) also captures the radial dynamics of a meandering spiral.

In the numerical simulations the moving source initially modulates the local wave number which subsequently leads to a modulation of the wave amplitude. For large r (far field), we observe modulations with a period T that is equal to the forcing period τ and independent from R_S. First, we forced sources (respectively, "spirals") in the parameter region where $q_S < q_E$; in this case the perturbation is always damped out while the waves move away from the source. A larger variety of responses occurs in the convectively Eckhaus unstable regime, where the unperturbed source selects a wave number q_S in the interval $[q_E, q_A]$. Figure 2 shows three qualitatively different resulting profiles of the amplitude $|A|$ as a function of the radial coordinate. Figures 2(a)–2(c) correspond to increasing values of the forcing period τ. For small τ values, the result is similar to the case with $q_S < q_E$, and the amplitude modulation is exponentially damped and is barely visible at sufficiently large r [Fig. 2(a)]. For intermediate τ, the amplitude modulation first grows and then reaches saturation [Fig. 2(b)]. The profile of $|A|$ is periodic and travels with a nonzero velocity; in the far field, the radial dynamics resemble a so-called modulated amplitude wave (see below). Finally for large τ, the amplitude modulation grows monotonically with r and space-time defects are formed at the breakup radius $r = R_{\mathrm{BU}} \approx 950$ [Fig. 2(c)]. For simulations with $q_S > q_A$, we always observe monotonic growth of the modulation leading to space-time defects.

A drawback of the homogeneous CGLE in 2D is that it does not support meandering spirals. A nonsaturating meandering instability has been observed for large values of c_1 [15]. Alternatively, the addition of a heterogeneity near the spiral core leads to meandering behavior similar to the one typically seen in reaction-diffusion systems [16]. Figures 1(e) and 1(f) show such a superspiral. The corresponding quantities for a regular spiral are shown in Figs. 1(b) and 1(c). As in Fig. 2(b) and in the recent experiment by Zhou and Ouyang [see Fig. 1(d) and [8]] the amplitude modulation shown in Fig. 1(f) saturates in the far field. To summarize, periodically moving sources emit modulated amplitude waves analogous to the way stationary sources emit plane waves. In the following, the study will be limited to the radial dynamics.

Modulated amplitude waves (MAWs) and superspirals.—MAWs are solutions of the CGLE and have the form

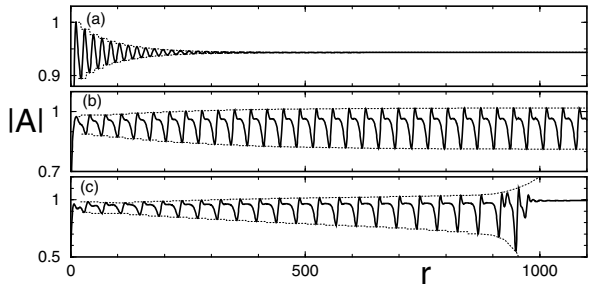

FIG. 2. Doppler effect of nonlinear waves due to periodic oscillations of the source at the left boundary. Equation (1) was integrated for increasing forcing periods (a) $\tau = 8$, (b) $\tau = 13$, (c) $\tau = 15$ with Eq. (5) and $c_1 = 3.5$, $c_3 = 0.4$, $R_S = 1$. Dotted lines are guides to the eye that converge to $|A|_{\min}$ and $|A|_{\max}$ in (b).

$$A(r, t) = a(z)e^{i\phi(z)}e^{i(qr-\omega t)}, \quad (6)$$

with periodic functions a and ϕ of the comoving coordinate $z = r - vt$ [17]. The analysis of MAWs has revealed that they bifurcate from plane waves with $q > q_E$. MAWs form a two-parameter family of waves described by the wavelength P of the modulation of the amplitude $a = |A|$ and by the spatially averaged phase gradient $\nu = q + \langle \partial_r \phi \rangle$. The velocity v and the period $T = P/v$ can be derived from these quantities. The average phase gradient is conserved as long as no space-time defect is formed. For periodically perturbed sources, the phase gradient value is fixed to $\nu \equiv q_S$. Therefore, only one free parameter is left. For the present purpose it is most convenient to use the period T. The bifurcation diagram has been computed via Newton's method applied to coherent structures that are exact solutions of the system of ordinary differential equations resulting from the insertion of the ansatz (6) into the CGLE (1) [17,18]. The results of this numerical bifurcation analysis are denoted by solid and dashed curves in Fig. 3 for the case $q_S > q_E$ (Eckhaus unstable range). Stable MAWs do not exist for $q_S < q_E$.

Figure 3 reveals that stable MAWs exist for periods T in the interval $[T_{\mathrm{HB}}, T_{\mathrm{SN}}]$. They are "born" in a Hopf bifurcation (HB) and "die" in a saddle-node bifurcation (SN). For $T < T_{\mathrm{HB}}$, the plane wave is stable and for $T > T_{\mathrm{SN}}$ no MAWs exist and the dynamics leads to the formation of defects [17,19]. This clarifies our findings in Fig. 2: the profiles in Figs. 2(a)–2(c) correspond to forcing within the regions $\tau < T_{\mathrm{HB}}$, $T_{\mathrm{HB}} < \tau < T_{\mathrm{SN}}$, and $T_{\mathrm{SN}} < \tau$, respectively. Figure 3(b) shows the breakup radius R_{BU} found in simulations for periods $\tau > T_{\mathrm{SN}}$. It is crucial to realize that the properties of the saturated modulations, observed in numerical simulations with a periodically moving source, indeed correspond to the MAWs with $\nu = q_S$ and $T = \tau$ computed via a bifurcation analysis (as shown in Fig. 3). Thus, a unique MAW characterized by two parameters is selected in 1D by the BC in Eq. (6) or in 2D by the two intrinsic frequencies of a meandering spiral. We conjecture that the bifurcation diagram of superspirals in 2D can be predicted from the corresponding bifurcation diagram of the far-field MAWs provided the meandering period (that here corresponds to τ) is known. Hence, the superspirals with saturated modulation should cease to exist in the saddle-node bifurcation of the associated MAW. If $\tau > T_{\mathrm{SN}}$, the modulations grow monotonic and form space-time defects in 1D, respectively, topological defects in 2D (spiral breakup). In explicit 2D simulations, such behavior has already been observed in a homogeneous reaction-diffusion model for calcium waves, where simultaneous appearance of the Eckhaus instability and meandering leads to a breakup far away from the spiral core [20]. Future studies may address the possibility of MAWs in realistic reaction-diffusion systems which exhibit Eckhaus instabilities [20,21].

A previous linear analysis of superspirals predicted that the meandering instability of a spiral with an Eckhaus unstable wave train in the far field may produce superspirals with exponentially growing modulation, while in the standard case of a meandering spiral emitting a stable wave train exponential damping of the modulation should be observed [7]. Our numerical nonlinear analysis introduces superspirals with a saturated modulation in the far field as a third possibility, thus supporting the experimental observation of such structures in the BZ reaction (Fig. 1

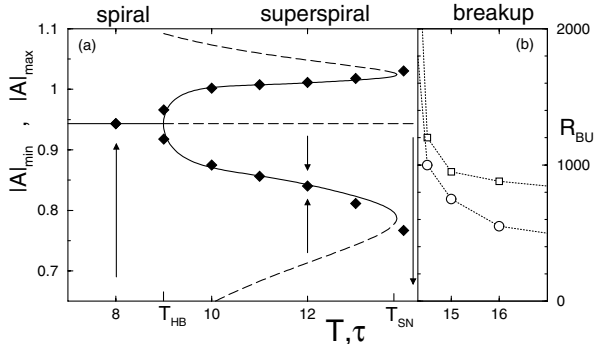

FIG. 3. (a) Bifurcation diagram for MAWs with period T and existence domains of spirals, superspirals, and spiral breakup for various forcing periods τ. Curves were numerically computed by bifurcation analysis as in [17,18] and symbols denote minima and maxima of $|A|$ as measured in simulations; parameters are the same as in Fig. 2. Solid (dashed) curves correspond to stable (unstable) solutions. Arrows (same for $|A|_{\mathrm{max}}$) indicate the evolution of initial perturbations as they move away from the source. Their asymptotic values depend on $T = \tau$ but not on R_S. (b) Breakup radius R_{BU} at which defects first occur in simulations. Smaller remaining spirals result from larger R_S ($R_S = 5$ circles, $R_S = 1$ squares).

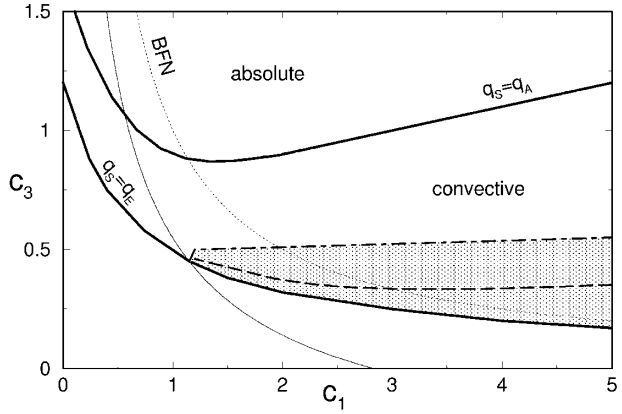

FIG. 4. Phase diagram indicating the region (shaded) where superspirals may occur in the CGLE for "rocking" sources. Simple spirals with selected $q_S(c_1, c_3)$ are convectively unstable between the thick solid curves. Superspiral breakup is only possible between the dashed and dash-dotted curves. The Eckhaus instability for arbitrary q is supercritical above the thin solid curve and the thin dotted curve indicates the Benjamin-Feir-Newell line (BFN).

and [7]). We suggest an interpretation of the reported scenario damped superspiral — saturated superspiral — far-field breakup: the three phenomenologies simply correspond to the three mentioned regions of the bifurcation diagram for the MAWs. Notice, bifurcation diagrams similar to Fig. 3(a) are found when c_1 or c_3 are varied at fixed T [17–19].

Phase diagram.—Finally we determine the regions of the c_1-c_3 phase diagram [12] where the discussed phenomena may be found. The results of the fully nonlinear bifurcation analysis are summarized in Fig. 4 where ν is fixed equal to $q_S(c_1, c_3)$ as given by Eq. (4). Saturated superspirals can appear only above the Eckhaus line for $q_S > q_E$. For small values of c_1, the MAWs bifurcate subcritically and are always unstable [22]. Figure 4 also shows the line of absolute instability ($q_S = q_A$) above which simple spirals break up giving rise to spatiotemporal chaos. Stable MAWs with $\nu = q_S$ do exist in the shaded region (for an extensive discussion on MAW stability see [18]). Below the thick dashed line in Fig. 4 no saddle-node bifurcation does occur and breakup is therefore prevented. Between the thick dashed and the thick dash-dotted lines in Fig. 4, bifurcation diagrams similar to Fig. 3(a) are found. In this region, all the three behaviors reported in Fig. 2 are possible, depending on the period of the forcing or meandering. Altogether, the results here presented link far-field breakup of meandering spirals to a saddle-node bifurcation. Thus, this route to spatiotemporal chaos can be distinguished from the previously reported scenario of far-field breakup caused by an absolute Eckhaus instability of the asymptotic far-field wave train [12,13,21,23].

Conclusions.—We have studied the Doppler effect associated with the back-and-forth motion of a source emitting periodic nonlinear waves. Usually, the resulting modulation dies out by exponential damping as the waves move away from the source. If the emitted wave train is convectively Eckhaus unstable, the wave modulation can also saturate or grow exponentially far away from the source depending on the period of the back-and-forth motion. These scenarios are fully determined by the bifurcation diagram of corresponding MAWs. Our results offer a consistent explanation of recent experimental results obtained in a chemical reaction [8]. Moreover, they may find application in future studies of other experimental systems exhibiting convective instabilities like hydrothermal waves [24]. Periodic forcing of sources near the transition to chaotic dynamics may be used to probe the existence and properties of modulated structures.

We acknowledge stimulating discussions with B. Sandstede and Q. Ouyang. In addition we would like to thank Q. Ouyang for the permission to report his experimental images in Figs. 1(a) and 1(d).

*Electronic address: torcini@ino.it
†Electronic address: baer@mpipks-dresden.mpg.de

[1] M. C. Cross and P. C. Hohenberg, Rev. Mod. Phys. **65**, 851 (1993); *Chemical Waves and Patterns*, edited by R. Kapral and K. Showalter (Kluwer, Dordrecht, 1994); J. Keener and J. Sneyd, *Mathematical Physiology* (Springer, New York, 1998).
[2] P. S. Hagan, SIAM J. Appl. Math. **42**, 762 (1982).
[3] Y. Kuramoto, *Chemical Oscillations, Waves and Turbulence* (Springer, Berlin, 1984).
[4] I. S. Aranson and L. Kramer, Rev. Mod. Phys. **74**, 99 (2002).
[5] A. S. Mikhailov, V. Davydov, and V. S. Zykov, Physica (Amsterdam) **70D**, 1 (1994); M. Bär *et al.*, J. Chem. Phys. **100**, 1202 (1994); R. M. Mantel and D. Barkley, Phys. Rev. E **54**, 4791 (1996).
[6] W. Jahnke, W. E. Skaggs, and A. T. Winfree, J. Phys. Chem. **93**, 740 (1989); T. Plesser, S. C. Müller, and B. Hess, J. Phys. Chem. **94**, 7501 (1990); G. S. Skinner and H. L. Swinney, Physica (Amsterdam) **48D**, 1 (1991); D. Barkley, Phys. Rev. Lett. **68**, 2090 (1992); G. Li *et al.*, Phys. Rev. Lett. **77**, 2105 (1996).
[7] B. Sandstede and A. Scheel, Phys. Rev. Lett. **86**, 171 (2001).
[8] L. Q. Zhou and Q. Ouyang, Phys. Rev. Lett. **85**, 1650 (2000); J. Phys. Chem. A **105**, 112 (2001).
[9] V. Perez-Munuzuri *et al.*, Nature (London) **353**, 740 (1991).
[10] E. Bodenschatz, A. Weber, and L. Kramer, in *Nonlinear Wave Processes in Excitable Media*, edited by A. V. Holden *et al.* (Plenum Press, New York, 1990).
[11] The function α is given by $\alpha(c_1, c_3) = \sqrt{f(c_1, c_3)/g(c_1, c_3)}$ with $f(c_1, c_3) = 3c_1[8(c_1 - c_3)^2 + 9(1 + c_1c_3)^2 - 4c_1c_3]^{1/2} + c_1(5 - 9c_1c_3) - 4c_3$ and $g(c_1, c_3) = 4(-2c_3 + 9c_1^3 + 7c_1)$.
[12] I. Aranson *et al.*, Phys. Rev. A **46**, 2992 (1992).
[13] S. M. Tobias and E. Knobloch, Phys. Rev. Lett. **80**, 4811 (1998); Physica (Amsterdam) **113D**, 43 (1998).
[14] D. Barkley, Phys. Rev. Lett. **72**, 164 (1994).
[15] I. Aranson, L. Kramer, and A. Weber, Phys. Rev. Lett. **72**, 2316 (1994).
[16] I. S. Aranson, L. Kramer, and A. Weber, in *Spatio-Temporal Patterns in Nonequilibrium Complex Systems*, edited by P. E. Cladis and P. Palffy-Muhoray (Addison-Wesley, Reading, 1995).
[17] L. Brusch *et al.*, Phys. Rev. Lett. **85**, 86 (2000); Physica (Amsterdam) **160D**, 127 (2001).
[18] L. Brusch, A. Torcini, and M. Bär, Physica (Amsterdam) **174D**, 152 (2003).
[19] M. van Hecke, Physica (Amsterdam) **174D**, 134 (2003).
[20] M. Falcke *et al.*, Physica (Amsterdam) **129D**, 236 (1999).
[21] M. Bär and M. Or-Guil, Phys. Rev. Lett. **82**, 1160 (1999); B. Sandstede and A. Scheel, Phys. Rev. E **62**, 7708 (2000).
[22] B. Janiaud *et al.*, Physica (Amsterdam) **55D**, 269 (1992).
[23] Q. Ouyang and J. M. Flesselles, Nature (London) **379**, 143 (1996).
[24] N. Garnier and A. Chiffaudel, Phys. Rev. Lett. **86**, 75 (2001); N. Garnier, A. Chiffaudel, and F. Daviaud, Physica (Amsterdam) **174D**, 30 (2003).